

1 APPLICATION

2 **Running head:** PAVO 2.0

3 pavo 2.0: new tools for the spectral and spatial  
4 analysis of colour in R

5 Rafael Maia<sup>1</sup>, Hugo Gruson<sup>2</sup>, John A. Endler<sup>3</sup> & Thomas E. White<sup>4,\*</sup>

6 <sup>1</sup> Department of Ecology, Evolution and Environmental Biology, Columbia Uni-  
7 versity, New York, NY 10027, U.S.A.

8 <sup>2</sup> CEFE, Univ Montpellier, CNRS, Univ Paul Valery Montpellier 3, EPHE, IRD,  
9 Montpellier, France

10 <sup>3</sup> School of Life and Environmental Sciences, Deakin University, Waurin Ponds  
11 campus, VIC, 3216, Australia.

12 <sup>4</sup> School of Life and Environmental Sciences, University of Sydney, Sydney, NSW,  
13 2006, Australia

14 \* corresponding author: `thomas.white@sydney.edu.au`

15 **Keywords:** colour, vision, spectra, spectrometry, photography, colourspace, re-  
16 flectance, sensory ecology

## 17 **Abstract**

18 1. Biological colouration presents a canvas for the study of ecological and  
19 evolutionary processes. Enduring interest in colour-based phenotypes has  
20 driven, and been driven by, improved techniques for quantifying colour pat-  
21 terns in ever-more relevant ways, yet the need for flexible, open frameworks  
22 for data processing and analysis persists.

23 2. Here we introduce `pavo 2.0`, the latest iteration of the R package `pavo`. This  
24 release represents the extensive refinement and expansion of existing meth-  
25 ods, as well as a suite of new tools for the cohesive analysis of the spectral  
26 and (now) spatial structure of colour patterns and perception. At its core,  
27 the package retains a broad focus on (a) the organisation and processing of  
28 spectral and spatial data, and tools for the alternating (b) visualisation, and  
29 (c) analysis of data. Significantly, `pavo 2.0` introduces image-analysis ca-  
30 pabilities, providing a cohesive workflow for the comprehensive analysis of  
31 colour patterns.

32 3. We demonstrate the utility of `pavo` with a brief example centred on mimicry  
33 in *Heliconius* butterflies. Drawing on visual modelling, adjacency, and bound-  
34 ary strength analyses, we show that the combined spectral (colour and lu-  
35 minance) and spatial (pattern element distribution and boundary salience)  
36 features of putative models and mimics are closely aligned.

37 4. `pavo 2.0` offers a flexible and reproducible environment for the analysis of  
38 colour, with renewed potential to assist researchers in answering fundamen-  
39 tal questions in sensory ecology and evolution.

## 40 Introduction

41 The study of colour in nature continues to generate fundamental knowledge:  
42 from the neurobiology and ecology of information processing (Caves *et al.*, 2018;  
43 Schnaitmann *et al.*, 2018; Thoen *et al.*, 2014; White & Kemp, 2017), to the evolution-  
44 ary drivers of life's diversity (Dalrymple *et al.*, 2015, 2018; Endler, 1980; Maia *et al.*,  
45 2013b). Colour is a subjective perceptual experience, however, so our understand-  
46 ing of the function and evolution of this conspicuous facet of variation depends  
47 on our ability to analyse phenotypes in meaningful ways. Excellent progress con-  
48 tinues to be made in this area, with emerging techniques now able to quantify and  
49 integrate both the spectral (i.e. colour and luminance) and spatial (i.e. the dis-  
50 tribution of pattern elements) properties of colour patterns (Endler, 2012; Endler  
51 *et al.*, 2018; Kemp *et al.*, 2015; Renoult *et al.*, 2015; Troscianko *et al.*, 2017). The need  
52 remains, however, for tools that integrate these complex methods into clear, open,  
53 and reproducible workflows (White *et al.*, 2015), allowing researchers to retain  
54 focus on the exploration of interesting questions.

55 Here we introduce pavo 2.0, a major revision and update of the R package  
56 pavo (Maia *et al.*, 2013a). Since its initial release, the package has provided a  
57 cohesive framework for the processing and analysis of spectral data, yet the inter-  
58 ceding years have seen the advent of novel analytical methods and the refinement  
59 of existing ones. As detailed below, pavo 2.0 has been extensively expanded to  
60 incorporate a suite of new tools, with the most significant advance being the in-  
61 clusion of geometry-based analyses. This allows for the quantification of spectral  
62 and spatial properties of colour patterns within a single workflow, thereby min-  
63 imising the computational and cognitive overhead associated with their otherwise  
64 fragmented analysis.

## 65 **The pavo package, version 2.0**

66 The conceptual focus of pavo remains centred on three components: (1) data  
67 importing and processing, and ongoing feedback between (2) visualisation and  
68 (3) analysis (Fig. 1). The package is available for direct installation through  
69 R from CRAN (<https://CRAN.R-project.org/package=pavo>), while the devel-  
70 opment version remains available on Github (<https://github.com/rmaia/pavo>).  
71 Comprehensive details and examples of the rich functionality of pavo are avail-  
72 able in help files as well as the package vignettes. Indeed, we strongly encour-  
73 age readers to refer to the vignettes as the primary source for information on  
74 pavo's functionality (accessible through `browseVignettes(pavo)`, and at [http://](http://rafaelmaia.net/pavo/)  
75 [rafaelmaia.net/pavo/](http://rafaelmaia.net/pavo/)), since they are updated as necessary with every pack-  
76 age release.

## 77 **Organisation**

78 Images and spectra can be loaded into pavo in bulk through the use of `getimg` and  
79 `getspec`, respectively. Both are capable of handling multiple data formats, such  
80 as jpeg, bmp and png in the case of images, and over a dozen formats of spectral  
81 data, including the diverse and complex proprietary formats of the various spec-  
82 trometer vendors. Once loaded, the data are stored as objects of an appropriate  
83 custom S3 class, for use in further functions. Spectral data are of class `rspec`, and  
84 inherit methods from `data.frame`, while images are of class `getimg`, and are mul-  
85 tidimensional objects (typically 3D, for an RGB image) that inherits methods from  
86 `array`. If more than one image is imported in a single call to `getimg`, then each  
87 image is stored as an element of a `list`. This class system allows for — among  
88 other things — the reliable use of generic functions such as `plot` and `summary`,  
89 which can be called any time to inspect and visualise data.

90 Several functions then facilitate the initial processing of colour data. It is of-  
91 ten desirable to process spectra to remove unwanted noise, modify the spectral

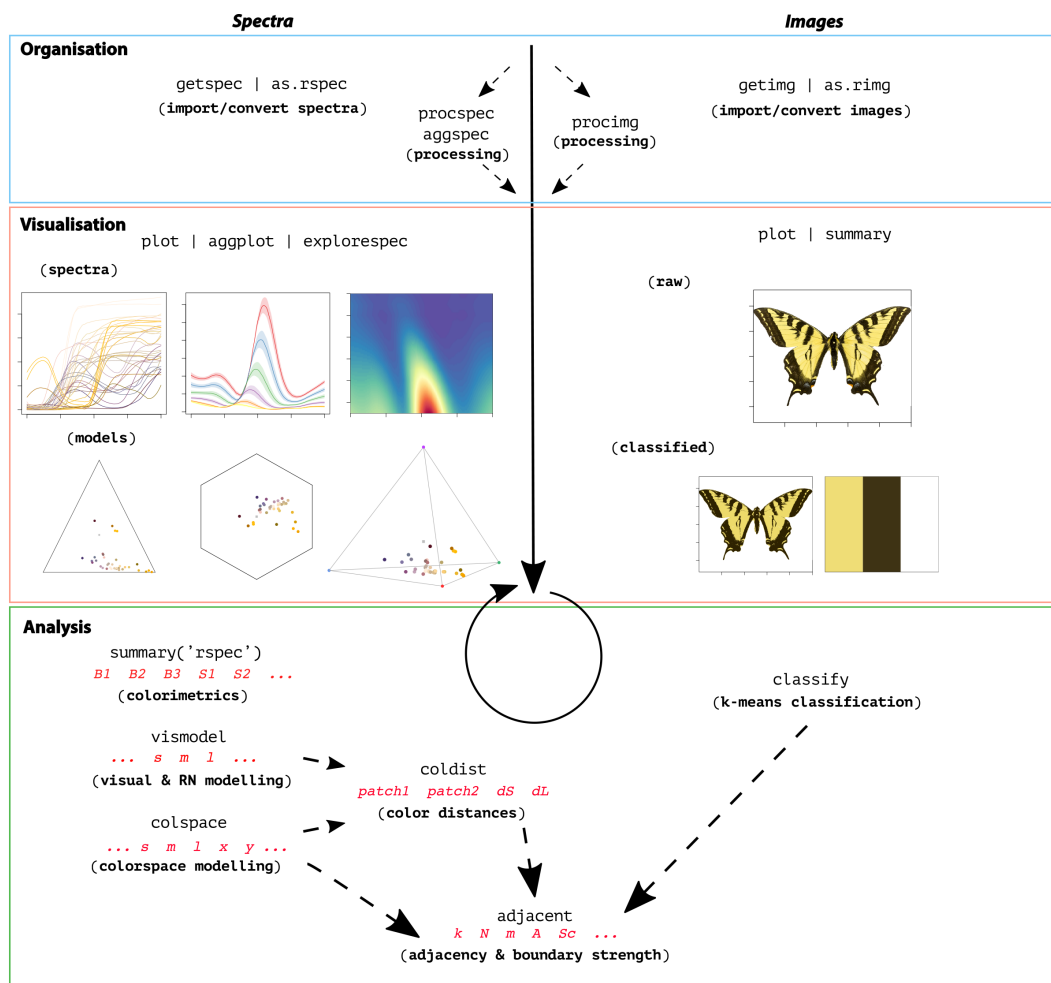


Figure 1: A general overview of the colour-pattern analysis workflow in pavo, as of version 2.0, displaying some key functions at each stage.

92 range, and/or interpolate the standard wavelength intervals, all of which may be  
 93 achieved through `procspec`. For images, `procimg` offers similar functionality such  
 94 as the ability to interactively specify the real-world scale of images (in preferred  
 95 units of measurement), rotate and resize images, or define the boundary between  
 96 a focal object and the visual background. The scope of image processing in pavo  
 97 2.0 is relatively limited by design, as much of what might be used during standard  
 98 image handling are either needs best considered and met by researchers during  
 99 image capture and data-checking, or are readily achieved within R using existing  
 100 packages such as `imager` (Barthelme, 2018) and `magick` (Ooms, 2018). Indeed, pavo  
 101 2.0 includes two convenience functions, `ring2cimg` and `cimg2ring`, to convert be-

102 tween image-classes used by `pavo` and `imager`, allowing ready access to extensive  
103 image-processing capabilities.

## 104 **Visualisation**

105 The repeated visualisation of spectral and spatial data is an essential step during  
106 all stages of analysis, and `pavo 2.0` offers numerous tools and publication-ready  
107 graphics fit for purpose. Once the package is loaded, the `plot` function recognises  
108 objects of class `rspec` and `ring`, as well as `colspace` (the product of visual mod-  
109 elling, detailed below), and becomes the conduit to most visualisations. For raw  
110 spectral data, for example, `plot` will produce a clean plot of the spectra versus  
111 wavelengths (Fig. 1, centre-left). Following visual modelling, di-, tri-, and tetra-  
112 chromatic models can instead be visualised, as well as data from more specialised  
113 models, such as the colour hexagon (Chittka, 1992), CIEXYZ or LAB spaces (Smith  
114 & Guild, 1931; Westland *et al.*, 2012), categorical space (Troje, 1993), segment anal-  
115 ysis (Ender, 1990), the colour-opponent coding space (Backhaus, 1991), or the  
116 'receptor-noise' space (de Ibarra *et al.*, 2001; Pike, 2012). Images can also be plot-  
117 ted, with the result depending on whether and how they have been processed.  
118 When given an unprocessed `ring` object, `plot` will produce a simple raster-based  
119 plot of the image (Fig. 1, right). Following the results of `classify`, in which image  
120 pixels are k-means classified into discrete colour-classes (or if a colour-classified  
121 image is loaded directly), the plot will use the mean RGB values of each colour-  
122 class to plot the now-classified image (Fig. 2).

## 123 **Analysis**

124 Since the perception of colour is a subjective experience, significant progress has  
125 been made in representing its reception using ecologically relevant 'visual models'  
126 (Kelber *et al.*, 2003; Kemp *et al.*, 2015; Renoult *et al.*, 2015), which `pavo 2.0` includes  
127 in an extended repertoire. The first step in such analyses is a call to `vismodel`,

128 which models photoreceptor stimulation (quantum-catches, or photon-flux) based  
129 on information about the viewer's visual sensitivity and viewing environments.  
130 While users are free to use their own spectra, `pavo` includes a suite of built-in  
131 receptor sensitivities, illuminant and transmission data (be it environmental or  
132 ocular), and viewing backgrounds, for convenience.

133 Once quantum catches are estimated the results can be used in a number of mod-  
134 els, depending on the question and analytical objective at hand (Kemp *et al.*, 2015;  
135 Renoult *et al.*, 2015). General colourspaces are available through a call to `colspace`  
136 which, if provided no further arguments, will model the data in a generalist di-  
137 tri- or tetrachromatic space informed by the dimensionality of the visual system.  
138 More specialised colourspaces — which may be informed by specific information  
139 about the visual perception of particular species — are also available via `colspace`.  
140 The CIEXYZ, CIELAB, and CIELch models (designed and intended exclusively  
141 for humans) are available, and `colspace` will check that the appropriate inputs,  
142 such as the human colour-matching function, have been used to model receptor  
143 stimulation, as required (Smith & Guild, 1931; Westland *et al.*, 2012). The colour-  
144 opponent-coding (Backhaus, 1991) and colour-hexagon (Chittka, 1992) models of  
145 bee vision are implemented, as is the categorical model of fly colour-vision de-  
146 tailed by Troje (1993). Plots for every space are accessible through a call to `plot`  
147 which, thanks to the underlying class system, will draw on the appropriate vi-  
148 sualisation for the model at hand — be it a hexagon, a dichromatic segment, a  
149 Maxwell triangle, or a three-dimensional tetrahedron.

150 The receptor-noise limited model of early-stage (retinal) colour processing has  
151 proven exceptionally popular (Vorobyev *et al.*, 2001; Vorobyev & Osorio, 1998), and  
152 has been tested to varying degrees in diverse taxa (Barry *et al.*, 2015; Fleishman  
153 *et al.*, 2016; Kelber *et al.*, 2003; Olsson *et al.*, 2015; White & Kemp, 2016). Following  
154 the estimation of receptor stimulation in `vismodel`, the model incorporates infor-  
155 mation on relative receptor densities and noise through the function `coldist`, and  
156 estimates either quantum- or neural-noise weighted colour distances. Version 2.0

157 of pavo introduces several extensions of this approach, such as the bootstrapped  
158 colour distance of `bootcolldist`, which provides an estimate of the noise-weighted  
159 distances ( $\delta S$ 's and/or  $\delta L$ 's) between the centroids of colour samples in multivari-  
160 ate space, with an appropriate measure of error (Maia & White, 2018). Stimuli can  
161 also now be expressed and plotted as coordinates in 'perceptual' (i.e. receptor-  
162 noise corrected) space by calling `jnd2xyz` on the distances calculated in `colldist`  
163 (de Ibarra *et al.*, 2001; Pike, 2012). Notably, these functions accept n-dimensional  
164 data, allowing for the modelling of extreme (Chen *et al.*, 2016; Cronin & Marshall,  
165 1989) or hypothetical high-dimensional visual systems. Of course `colldist` also  
166 accepts the results of alternative models — such as the hexagon or CIELab — and  
167 will return colour distances in units appropriate for each space.

168       Exciting recent advances now allow for the analysis of colour pattern geometry  
169 — that is, the *spatial* structure of colour patches — in conjunction with the compar-  
170 atively well-developed approaches to the *spectral* analysis of colour outlined above  
171 (Endler, 2012; Endler *et al.*, 2018; Pike, 2018; Troscianko *et al.*, 2017). The most  
172 significant extension of pavo as of 2.0 is the introduction of an image-based work-  
173 flow to allow for the combined analysis of the spectral and spatial structure of  
174 colour patterns, currently centred on the adjacency analysis (Endler, 2012), its ex-  
175 tension, the boundary strength analysis (Endler *et al.*, 2018), and related measures  
176 of overall pattern contrast (Endler & Mielke, 2005). Briefly, this process entails  
177 classifying the pixels of images into a number of discrete colour classes, before  
178 sampling the now-classified image with an evenly spaced grid. The column-wise  
179 and row-wise colour-class transitions between adjacent points are then tallied, and  
180 from this a suite of summary statistics on pattern structure — from simple colour  
181 proportions, through to colour diversity and pattern complexity — are estimated  
182 (e.g. Endler *et al.*, 2014; Rojas *et al.*, 2014; Rojas & Endler, 2013). If the colour 'dis-  
183 tance' between adjacent colour classes is known, such as might be estimated using  
184 receptor-noise modelling above, then this can also be incorporated to derive sev-  
185 eral measures of the salience of patch boundaries, which are important for colour



186 pattern perception (discussed in [Endler \*et al.\*, 2018](#)). In `pavo 2.0`, these steps are  
187 carried out through calls to `classify`, which uses k-means clustering to automati-  
188 cally or interactively classify all image pixels into discrete colour-classes, followed  
189 by `adjacent`, which performs the adjacency analysis and, if appropriate colour  
190 distances are also specified, the boundary strength analysis.



Figure 2: A sample workflow for image handling and analysis in `pavo`, as of version 2.0. Images are first imported and optionally processed by, for example, setting scales (yellow line) or defining objects and backgrounds (red outline). They may then be colour-classified before being passed to analytical functions, currently centered on the adjacency and boundary-strength analyses. If backgrounds and focal objects are defined then they can be analysed separately, concurrently, or either one can be excluded entirely.

191 As alluded to earlier, our goal is to provide a flexible and relatively simple  
192 analytical framework for the analysis of a colour pattern's spatial structure us-  
193 ing images, without the need for specialised photographic equipment or and/or  
194 extensive calibration and processing (demonstrated in the colour-plate based ex-  
195 ample below). We thus make an analytical and conceptual distinction between  
196 the spectral data afforded by spectrometry, and the spatial data afforded by im-  
197 ages, with the two able to be conveniently combined during latter analyses (Fig.  
198 1). This also minimises the unnecessary duplication of efforts of more general-  
199 purpose tools such as `imager` ([Barthelme, 2018](#)) and `magick` ([Ooms, 2018](#)), and the

200 excellent image analysis toolbox for imageJ (Troscianko & Stevens, 2015), which  
201 offer rich functionality for image processing and (in the latter case) analysis.

## 202 **Worked example: mimicry in *Heliconius* spp.**

203 Butterflies of the genus *Heliconius* are widely involved in mimicry, and have proven  
204 an exemplary system for studies of colour pattern development, ecology, and evo-  
205 lution (Jiggins, 2016). Here we demonstrate some of pavo 2.0's capabilities by  
206 briefly examining the the visual basis of mimicry in this system, with the objective  
207 of quantifying the spectral and spatial (dis)similarity between putative models and  
208 mimics. For our spatial analyses, we follow Endler (2012) and use colour plate XII  
209 from Eltringham (1916), which is arranged into what he described as model and  
210 mimic pairs (Fig. 3). For our spectral analyses we collated six reflectance spec-  
211 tra from each of the the 'red', 'yellow', and 'black' patches of the forewings of two  
212 species — *H. egeria* and *H. melpomene* (Fig. 3, top left pair) — from personal sources  
213 and the literature (Bybee *et al.*, 2011; Wilts *et al.*, 2017). For reasons of simplicity  
214 and data availability we restrict our visual modelling to these two species, though  
215 the below spectral analyses would ideally be repeated for all model/mimic pairs.

### 216 ***Spectral analysis***

217 We first focus on the spectral data, since some of the results of this work will  
218 be drawn on for the latter pattern analyses. We begin by loading the reflectance  
219 spectra, which are saved in a single tab-delimited text file available at the package  
220 repository along with the image plates (<https://github.com/rmaia/pavo>), before  
221 LOESS-smoothing them to remove any minor electrical noise and zeroing spurious  
222 negative values.

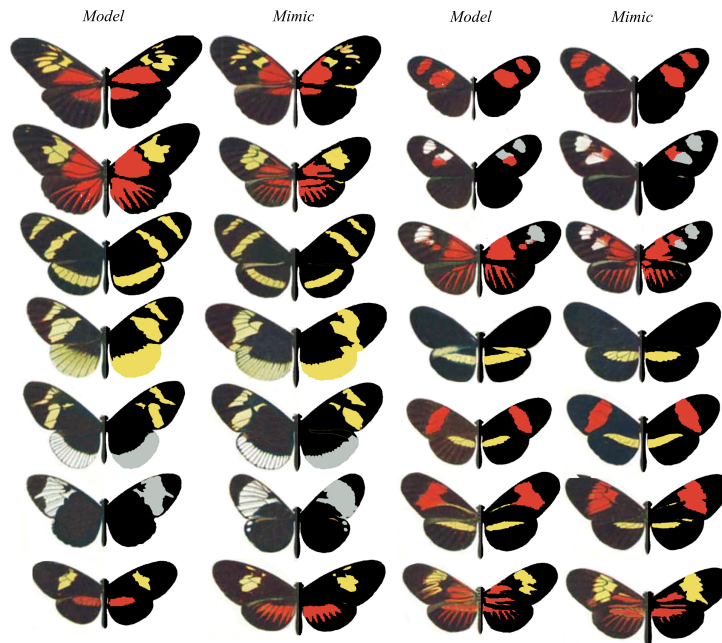


Figure 3: A modification of Eltringham's (1916) colour plate of *Heliconius* butterflies, *sensu* Endler (2012), arranged into putative models and mimics. The left side of each individual is as per the original, while the right half display pattern elements that have been classified into discrete classes through k-means clustering, using the `classify` function.

```
# Load spectra
```

```
> heli_specs <- getspec('../data', ext = 'txt')
```

```
# Smooth spectra and zero negative values
```

```
> heli_specs <- procspec(heli_specs,
```

```
>                               opt = 'smooth',
```

```
>                               fixneg = 'zero')
```

223 A call to `plot(heli_specs, col = spec2rgb(heli_specs))` displays the now-  
224 clean spectra, with each line coloured according to how it might appear to a hu-  
225 man viewer (Fig. 4, top left).

226 Since our interest is in quantifying the fidelity of visual mimicry, we must  
227 consider the perspective of ecologically relevant viewers (the primary selective  
228 agents) which, in the case of aposematic *Heliconius*, are avian predators (Benson,

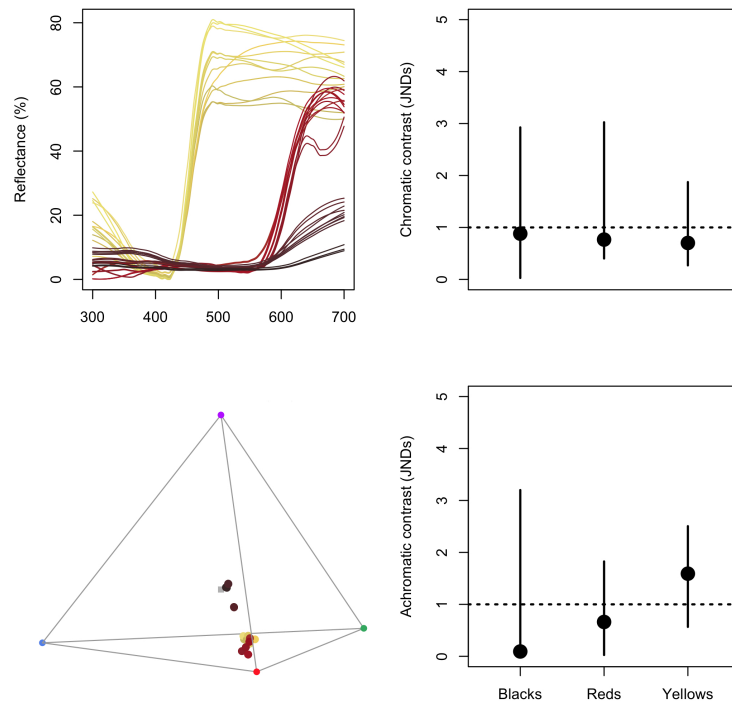


Figure 4: Reflectance spectra from black, red, and yellow patches of *H. egeria* and *H. melpomene*, along with their positions in a tetrahedral model of avian vision (left side). The bootstrapped, noise-corrected chromatic and achromatic patch distances between species (right) predicts that the individual colours of this model/mimic pair are likely indistinguishable to avian predators.

229 1972; Chai, 1986). We thus use the receptor-noise limited model (Vorobyev *et al.*,  
230 2001; Vorobyev & Osorio, 1998) to predict whether the black, red, and yellow  
231 colour patches of a representative model and mimic are distinguishable to avian  
232 predators. This first entails estimating the photoreceptor quantum catches of a  
233 representative viewer, so we use a built-in average UV-sensitive avian visual phe-  
234 notype for estimating chromatic distances, and the double-cone sensitivity of the  
235 blue tit for luminance distances.

```
> heli_model <- vismodel(heli_specs,  
>                       visual = 'avg.uv',  
>                       achromatic = 'bt.dc',  
>                       relative = FALSE)
```

236 At this point we may wish to get a quick sense of the relative distribution

237 of stimuli by converting them to locations in an avian tetrahedral colourspace  
238 and plotting the results with `plot(colspace(heli_model))` (Fig. 4). With receptor  
239 stimulation estimated, we now calculate noise-corrected chromatic and achromatic  
240 distances between patches. The `coldist` function can be used to return the pair-  
241 wise distances between every spectrum, which might then be averaged to derive  
242 a mean distance between species for every patch. This neglects the multivariate  
243 structure of such data, however, when the objective is to estimate the separation of  
244 groups in colour space (Maia & White, 2018). We therefore prefer a bootstrapped  
245 measure of colour distance using `bootcolldist`, which provides a robust measure  
246 of the separation of our focal samples (i.e the red, white, and black patches of  
247 model versus mimic), along with a 95% confidence interval, which can be in-  
248 spected to see if it exceeds the theoretical discrimination threshold of one JND. We  
249 specify a relative receptor density of 1:2:2:4 (ultraviolet:short:medium:long wave-  
250 length receptors; Maier & Bowmaker (1993)), a signal-to-noise ratio yielding a  
251 Weber fraction of 0.1 for both chromatic and achromatic receptors, and assume  
252 that noise is proportional to the Weber fraction and independent of the magnitude  
253 of receptor stimulation (reviewed in Kelber *et al.* (2003); Olsson *et al.* (2017)).

```
# Calculate the bootstrapped, noise-corrected colour distance  
# between groups, using sample names to specify grouping ID's.  
> heli_dist <- bootcolldist(heli_model,  
>                               by = sub('\\.*', '', rownames(heli_model)),  
>                               n = c(1, 2, 2, 4),  
>                               weber = 0.1,  
>                               weber.achro = 0.1)
```

254 Inspection of the key comparisons of interest (Fig. 4, right) reveals that the 95%  
255 CI of all chromatic and achromatic comparisons includes the theoretical threshold  
256 of one JND. This predicts that the individual colour pattern elements of putative  
257 model and mimic *H. egeria* and *H. melpomene* are indistinguishable, or difficult to

258 discriminate, to avian viewers — the assumed intended recipient of the aposematic  
259 signals. As noted above, the analysis of this representative pair can be readily  
260 scaled to encompass all species given the necessary data, and we can now use this  
261 information to inform our study of the spatial structure of these signals.

### 262 *Pattern analysis*

263 We first load the focal images, which comprise the individual samples from plate  
264 XII of Eltringham (1916), saved as jpegs (Fig. 3). We then plot one or all of the  
265 images to check they are as expected.

```
# Load all images. Here the 28 jpegs are stored in a folder called  
# 'butterflies' located within the current working directory.
```

```
> heli_images <- getimg("butterflies")
```

```
28 files found; importing images.
```

```
# Plot the first image in the list only.
```

```
> plot(heli_images[[1]])
```

```
# Plot all images, which will progress through
```

```
# the sequence automatically.
```

```
> plot(heli_images)
```

266 We then classify the pixels of all images into discrete colour or luminance cat-  
267 egories, here using k-means clustering, to create a colour-classified image matrix.  
268 The function `classify` will carry this out, though there are numerous specific  
269 ways in which it may be achieved, including automatically or 'interactively', with  
270 the option of a reference image as template. Since our images are heterogeneous,  
271 it is simplest to use the interactive version of `classify`, which will cycle through  
272 each image and ask the user to manually identify a sample from every discrete  
273 colour or luminance class present, which are then used as cluster centres.

```
# Interactively colour-classify all images using k-means clustering.  
> heli_class <- classify(heli_images, interactive = TRUE)  
  
# Cycle through plots of the colour-classified images, alongside their  
# identified colour palettes.  
> summary(heli_class, plot = TRUE)
```

274 Finally, we use an adjacency analysis to estimate a suite of metrics describ-  
275 ing the structure and complexity of the colour pattern geometry of model and  
276 mimic *Heliconius*, and by including the visually-modelled colour distances esti-  
277 mated above, the output will include several measures of the salience of colour  
278 patch edges as part of the boundary strength analysis (Endler, 2012; Endler *et al.*,  
279 2018). We will exclude the white background since it is not relevant, simply by  
280 specifying the colour-category ID belonging to the homogeneous underlay. If the  
281 image was more complex, such as an animal in its natural habitat, we would in-  
282 stead interactively identify and separate the focal animal and background using  
283 procimg (e.g. Fig. 2, second panel).

```
# Construct and inspect a data.frame of pairwise colour and luminance  
# distances between all colour classes, constructed from the earlier  
# receptor-noise modelled estimates. Note that we do not bother  
# including colour-class ID 1, since that is the white background  
# which is to be excluded from the analysis (see below).  
# (Alternatively we could include it, and it would simply be ignored).  
> distances <- data.frame(c1 = c(2, 2, 3),  
                          c2 = c(3, 4, 4),  
                          dS = c(10.6, 5.1, 4.4),  
                          dL = c(1.1, 2.5, 3.2))  
  
> distances  
c1 c2 dS dL
```

```
2   3   10.50  7.41
2   4   11.76  23.40
3   4   13.29  15.99

# Calculate adjacency and boundary-strength statistics. We specify a
# scale of 50 mm, and note that the 'white' background, which has a class
# ID of 1 in this case, is to be excluded from the analysis.
# We also include the colour distance between all patches, as estimated above.
> heli_adj <- adjacent(heli_class,
>
>                   xscale = 50,
>                   bkgID = 1,
>                   exclude = 'background',
>                   coldists = distances)

# Inspect a subset of the resulting data.frame. Variable meanings
# are detailed in the function documentation (see ?adjacent),
# or Endler (2012), Endler et al. (2018), and Endler & Mielke (2005).
> head(heli_adj)[, 1:7]
      k  N      n_off  p_2   p_3   p_4   q_2_2  ...
mimic_01 3 345522  6547  0.801  0.130  0.067  0.796
mimic_02 2 1018370 4091  0.835  0.164  NA      0.834
mimic_03 3 265278  6155  0.685  0.198  0.116  0.677
...
```

284 We can now inspect the pattern descriptors of particular interest, and explore  
285 the similarity of models and mimics with respect to their broader colour pattern  
286 geometry. As seen in Fig. 5, the relative proportions of focal colours (top row),  
287 measures of pattern diversity and complexity (centre row), and the salience of  
288 patch boundaries (bottom row) are highly correlated between species pairs. This,  
289 in conjunction with the above modelling, suggests that the overall colour pat-



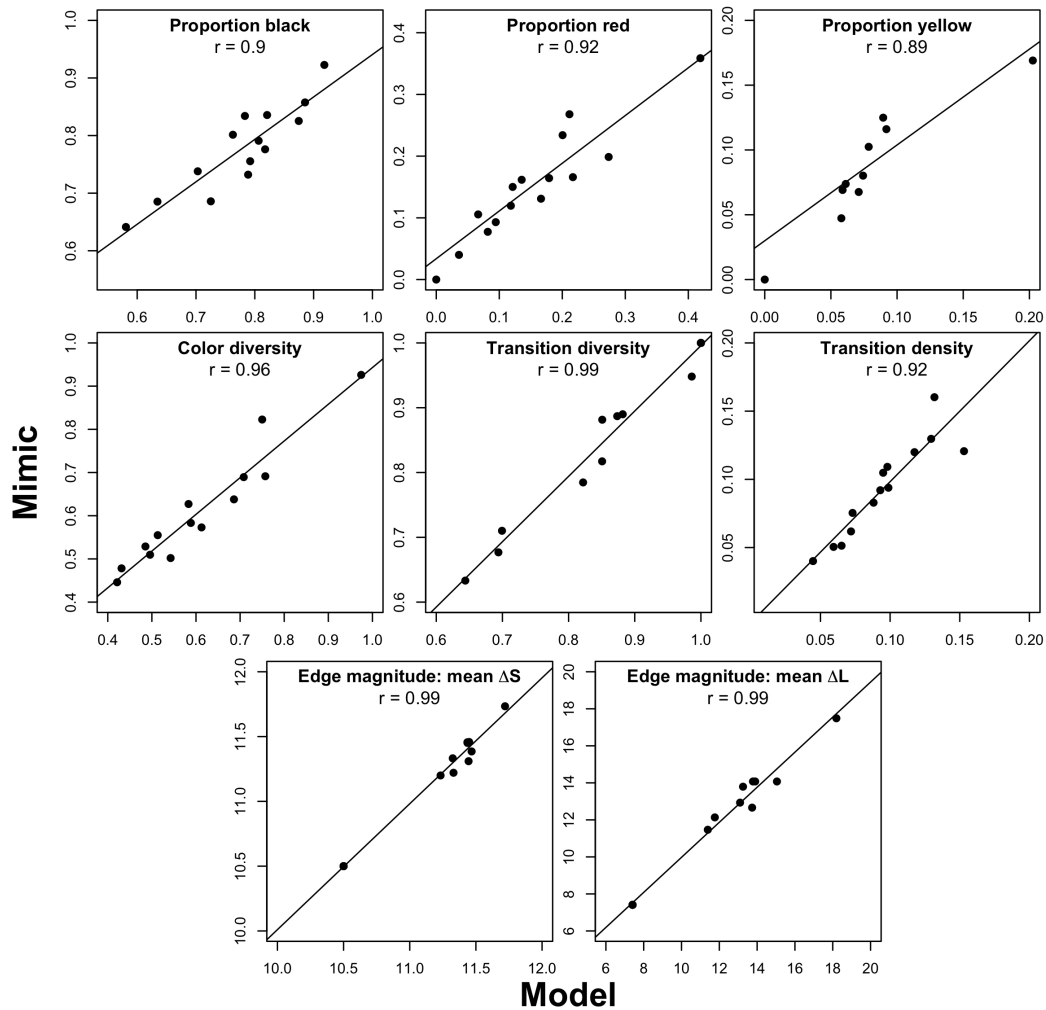


Figure 5: Select results of the colour pattern analysis of model and mimic *Heliconius* (Fig. 3), using adjacency and boundary strength analyses. Strong correlations are evident in colour proportions (top row), measures of colour diversity and complexity (centre row), and estimates of mean chromatic and achromatic edge salience (bottom row).

290 terns of putative model and mimic *Heliconius* — both spectrally and spatially —  
291 are highly similar, and are thus predicted to be very difficult to discriminate to  
292 the intended avian viewers of their aposematic signals, as consistent with theory  
293 (Müller, 1879). More interesting questions remain, of course, including the degree  
294 to which mimics need resemble models to deceive viewers, and the relative impor-  
295 tance of different colour pattern elements (e.g. Fig. 5) in mediating the subjective  
296 resemblance of species pairs, for which pavo is well suited to help answer.

## 297 **Conclusions**

298 The integrative study of biological colouration has borne rich fruit, though its po-  
299 tential to illuminate the structure and function of much of the natural world is not  
300 nearly realised (Endler & Mappes, 2017). As we have sought to demonstrate, pavo  
301 2.0 (and beyond) provides a flexible framework to assist researchers studying  
302 the physiology, ecology, and evolution of colour patterns and visual perception.  
303 We appreciate bug reports and suggestions, via email or the Github issue tracker  
304 <https://github.com/rmaia/pavo/issues>.

## 305 **Citation of methods**

306 Many of the methods applied in pavo are described in detail in their original  
307 publications — as listed in the documentation for the relevant functions — to  
308 which users should refer and cite as appropriate, along with pavo itself, via this  
309 publication (as of v2.0).

## 310 **Acknowledgements**

311 We thank Kate Umbers, Georgia Binns, and Julia Riley for the rigorous testing of  
312 image-based methods. TEW thanks Elizabeth Mulvenna and Cormac White for  
313 their support. The authors have no conflicts of interest to declare.

## 314 **Authors statement**

315 TEW, RM, and HG authored the software and manuscript, JAE developed and  
316 assisted in the implementation of methods, and critically revised the manuscript.

## 317 **References**

- 318 Backhaus, W. (1991) Color opponent coding in the visual system of the honeybee.  
319 *Vision research*, **31**, 1381–1397.
- 320 Barry, K.L., White, T.E., Rathnayake, D.N., Fabricant, S.A. & Herberstein, M.E.  
321 (2015) Sexual signals for the colour-blind: cryptic female mantids signal quality  
322 through brightness. *Functional Ecology*, **29**, 531–539.
- 323 Barthelme, S. (2018) *imager: image processing library based on CImg*. CRAN. R  
324 package version 0.41.1.
- 325 Benson, W.W. (1972) Natural selection for millerian mimicry in *Heliconius erato*  
326 in Costa Rica. *Science*, **176**, 936–939.
- 327 Bybee, S.M., Yuan, F., Ramstetter, M.D., Llorente-Bousquets, J., Reed, R.D., Osorio,  
328 D. & Briscoe, A.D. (2011) UV photoreceptors and UV-yellow wing pigments in  
329 *Heliconius* butterflies allow a color signal to serve both mimicry and intraspecific  
330 communication. *The American Naturalist*, **179**, 38–51.
- 331 Caves, E.M., Green, P.A., Zippel, M.N., Peters, S., Johnsen, S. & Nowicki, S. (2018)  
332 Categorical perception of colour signals in a songbird. *Nature*, p. 1.
- 333 Chai, P. (1986) Field observations and feeding experiments on the responses of  
334 rufous-tailed jacamars (*Galbula ruficauda*) to free-flying butterflies in a tropical  
335 rainforest. *Biological Journal of the Linnean Society*, **29**, 161–189.
- 336 Chen, P.J., Awata, H., Matsushita, A., Yang, E.C. & Arikawa, K. (2016) Extreme  
337 spectral richness in the eye of the common bluebottle butterfly, *Graphium sarpedon*.  
338 *Frontiers in Ecology and Evolution*, **4**, 18.
- 339 Chittka, L. (1992) The colour hexagon: a chromaticity diagram based on photore-  
340 ceptor excitations as a generalized representation of colour opponency. *Journal*  
341 *of Comparative Physiology A*, **170**, 533–543.

- 342 Cronin, T.W. & Marshall, N.J. (1989) A retina with at least ten spectral types of  
343 photoreceptors in a mantis shrimp. *Nature*, **339**, 137.
- 344 Dalrymple, R., Kemp, D., Flores-Moreno, H., Laffan, S., White, T., Hemmings, F.,  
345 Tindall, M. & Moles, A. (2015) Birds, butterflies and flowers in the tropics are not  
346 more colourful than those in higher latitudes. *Global Ecology and Biogeography*,  
347 pp. 848–860.
- 348 Dalrymple, R.L., Flores-Moreno, H., Kemp, D.J., White, T.E., Laffan, S.W., Hem-  
349 mings, F.A., Hitchcock, T.D. & Moles, A.T. (2018) Abiotic and biotic predictors of  
350 macroecological patterns in bird and butterfly coloration. *Ecological Monographs*,  
351 **88**, 204–224.
- 352 de Ibarra, N.H., Giurfa, M. & Vorobyev, M. (2001) Detection of coloured patterns  
353 by honeybees through chromatic and achromatic cues. *Journal of Comparative*  
354 *Physiology A*, **187**, 215–224.
- 355 Eltringham, H. (1916) Iv. on specific and mimetic relationships in the genus heli-  
356 conius, l. *Ecological Entomology*, **64**, 101–148.
- 357 Endler, J.A. & Mielke, P.W. (2005) Comparing entire colour patterns as birds see  
358 them. *Biological Journal of the Linnean Society*, **86**, 405–431.
- 359 Endler, J.A. (1980) Natural selection on color patterns in poecilia reticulata. *Evolu-*  
360 *tion*, **34**, 76–91.
- 361 Endler, J.A. (1990) On the measurement and classification of colour in studies of  
362 animal colour patterns. *Biological Journal of the Linnean Society*, **41**, 315–352.
- 363 Endler, J.A. (2012) A framework for analysing colour pattern geometry: adjacent  
364 colours. *Biological Journal of the Linnean Society*, **107**, 233–253.
- 365 Endler, J.A., Cole, G.L. & Kranz, X. (2018) Boundary strength analysis: Combin-  
366 ing colour pattern geometry and coloured patch visual properties for use in  
367 predicting behaviour and fitness. *Methods in Ecology and Evolution*, **Early View**.

- 368 Endler, J.A., Gaburro, J. & Kelley, L.A. (2014) Visual effects in great bowerbird sex-  
369 ual displays and their implications for signal design. *Proc R Soc B*, **281**, 20140235.
- 370 Endler, J.A. & Mappes, J. (2017) The current and future state of animal coloration  
371 research. *Phil Trans R Soc B*, **372**, 20160352.
- 372 Fleishman, L.J., Perez, C.W., Yeo, A.I., Cummings, K.J., Dick, S. & Almonte, E.  
373 (2016) Perceptual distance between colored stimuli in the lizard *anolis sagrei*:  
374 comparing visual system models to empirical results. *Behavioral Ecology and*  
375 *Sociobiology*, pp. 1–15.
- 376 Jiggins, C.D. (2016) *The ecology and evolution of Heliconius butterflies*. Oxford Uni-  
377 versity Press.
- 378 Kelber, A., Vorobyev, M. & Osorio, D. (2003) Animal colour vision – behavioural  
379 tests and physiological concepts. *Biological Reviews*, **78**, 81–118.
- 380 Kemp, D.J., Herberstein, M.E., Fleishman, L.J., Endler, J.A., Bennett, A.T.D., Dyer,  
381 A.G., Hart, N.S., Marshall, J. & Whiting, M.J. (2015) An integrative framework  
382 for the appraisal of coloration in nature. *The American Naturalist*, **185**, 705–724.
- 383 Maia, R., Eliason, C.M., Bitton, P.P., Doucet, S.M. & Shawkey, M.D. (2013a) pavo:  
384 an r package for the analysis, visualization and organization of spectral data.  
385 *Methods in Ecology and Evolution*, pp. 906–913.
- 386 Maia, R., Rubenstein, D.R. & Shawkey, M.D. (2013b) Key ornamental innovations  
387 facilitate diversification in an avian radiation. *Proceedings of the National Academy*  
388 *of Sciences*.
- 389 Maia, R. & White, T.E. (2018) Comparing colors using visual models. *Behavioral*  
390 *Ecology*, **29**, 649–659.
- 391 Maier, E.J. & Bowmaker, J.K. (1993) Colour vision in the passeriform bird, *leiothrix*  
392 *lutea*: correlation of visual pigment absorbance and oil droplet transmission  
393 with spectral sensitivity. *Journal of Comparative Physiology A*, **172**, 295–301.

- 394 Müller, F. (1879) Ituna and thyridia: a remarkable case of mimicry in butterflies.  
395 *Trans Entomol Soc Lond*, **1879**, 20–29.
- 396 Olsson, P., Lind, O. & Kelber, A. (2015) Bird colour vision: behavioural thresholds  
397 reveal receptor noise. *Journal of Experimental Biology*, **218**, 184–193.
- 398 Olsson, P., Lind, O. & Kelber, A. (2017) Chromatic and achromatic vision: param-  
399 eter choice and limitations for reliable model predictions. *Behavioral Ecology*, **29**,  
400 273–282.
- 401 Ooms, J. (2018) *magick: Advanced Graphics and Image-Processing in R*. CRAN. R  
402 package version 1.9.
- 403 Pike, T.W. (2012) Preserving perceptual distances in chromaticity diagrams. *Behav-*  
404 *ioral Ecology*, **23**, 723–728.
- 405 Pike, T.W. (2018) Quantifying camouflage and conspicuousness using visual  
406 salience. *Methods in Ecology and Evolution*.
- 407 Renoult, J.P., Kelber, A. & Schaefer, H.M. (2015) Colour spaces in ecology and  
408 evolutionary biology. *Biological Reviews*.
- 409 Rojas, B., Devillechabrolle, J. & Endler, J.A. (2014) Paradox lost: variable colour-  
410 pattern geometry is associated with differences in movement in aposematic  
411 frogs. *Biology letters*, **10**, 20140193.
- 412 Rojas, B. & Endler, J.A. (2013) Sexual dimorphism and intra-populational colour  
413 pattern variation in the aposematic frog *dendrobates tinctorius*. *Evolutionary*  
414 *Ecology*, **27**, 739–753.
- 415 Schnaitmann, C., Haikala, V., Abraham, E., Oberhauser, V., Thestrup, T., Gries-  
416 beck, O. & Reiff, D.F. (2018) Color processing in the early visual system of  
417 *drosophila*. *Cell*, **172**, 318–330.
- 418 Smith, T. & Guild, J. (1931) The cie colorimetric standards and their use. *Transac-*  
419 *tions of the optical society*, **33**, 73.

- 420 Thoen, H.H., How, M.J., Chiou, T.H. & Marshall, J. (2014) A different form of color  
421 vision in mantis shrimp. *Science*, **343**, 411–413.
- 422 Troje, N. (1993) Spectral categories in the learning behaviour of blowflies.  
423 *Zeitschrift fur Naturforschung C*, **48**, 96–96.
- 424 Troscianko, J., Skelhorn, J. & Stevens, M. (2017) Quantifying camouflage: how to  
425 predict detectability from appearance. *BMC evolutionary biology*, **17**, 7.
- 426 Troscianko, J. & Stevens, M. (2015) Image calibration and analysis toolbox—a free  
427 software suite for objectively measuring reflectance, colour and pattern. *Methods*  
428 *in Ecology and Evolution*, **6**, 1320–1331.
- 429 Vorobyev, M., Brandt, R., Peitsch, D., Laughlin, S.B. & Menzel, R. (2001) Colour  
430 thresholds and receptor noise: behaviour and physiology compared. *Vision*  
431 *Research*, **41**, 639–653.
- 432 Vorobyev, M. & Osorio, D. (1998) Receptor noise as a determinant of colour thresh-  
433 olds. *Proceedings of the Royal Society of London Series B: Biological Sciences*, **265**,  
434 351–358.
- 435 Westland, S., Ripamonti, C. & Cheung, V. (2012) *Computational colour science using*  
436 *MATLAB*. John Wiley & Sons.
- 437 White, T.E., Dalrymple, R.L., Noble, D.W.A., O’Hanlon, J.C., Zurek, D.B. & Um-  
438 bers, K.D.L. (2015) Reproducible research in the study of biological coloration.  
439 *Animal Behaviour*, **106**, 51–57.
- 440 White, T.E. & Kemp, D.J. (2016) Color polymorphic lures target different visual  
441 channels in prey. *Evolution*, **70**, 1398–1408.
- 442 White, T.E. & Kemp, D.J. (2017) Colour polymorphic lures exploit innate prefer-  
443 ences for spectral versus luminance cues in dipteran prey. *BMC evolutionary*  
444 *biology*, **17**, 191.

445 Wilts, B.D., Vey, A.J., Briscoe, A.D. & Stavenga, D.G. (2017) Longwing (helico-  
446 nius) butterflies combine a restricted set of pigmentary and structural coloration  
447 mechanisms. *BMC evolutionary biology*, **17**, 226.